

Article

Joint User Scheduling and Resource Allocation in Distributed MIMO Systems with Multi-Carriers

Yinglan Bu ¹, Jiaying Zong ², Xinjiang Xia ^{3,*}, Yang Liu ², Fengyi Yang ² and Dongming Wang ^{3,*}

¹ National Mobile Communications Research Laboratory, Southeast University, Nanjing 210096, China; buyl@seu.edu.cn

² China Telecom Research Institute, Beijing 102209, China; zongjy8@chinatelecom.cn (J.Z.); liuyang19@chinatelecom.cn (Y.L.); yangfy@chinatelecom.cn (F.Y.)

³ Purple Mountain Laboratories, Nanjing 211111, China

* Correspondence: xinjiang_xia@seu.edu.cn (X.X.); wangdm@seu.edu.cn (D.W.)

Abstract: Compared with the traditional collocated multi-input multi-output system (C-MIMO), distributed MIMO (D-MIMO) systems have the advantage of higher throughput and coverage, making them strong candidates for next-generation communication architecture. As a practical implementation of a D-MIMO cooperative network, the multi-TRP (multiple transmission/reception point) system becomes a hotspot in the research of advanced 5G. Different from previous research on a cooperative D-MIMO network with single narrowband transmission, this paper proposes a joint optimization scheme to address the user scheduling problem along with carrier allocation to maximize the total spectral efficiency (SE) in the downlink of coherent multi-TRP systems with multi-carriers. We establish a joint optimization model of user scheduling and resource allocation to maximize the system spectral efficiency under the constraints of power consumption and the backhaul capacity limits at each RAU (remote antenna unit), as well as the QoS (quality of service) requirement at each user. Since the optimization model is both non-convex and non-smooth, a joint optimization algorithm is proposed to solve this non-convex combinatorial optimization problem. We first smooth the mixed-integer problem by employing penalty functions, and after decoupling the coupled variables by introducing auxiliary variables, the original problem is transformed into a series of tractable convex optimization problems by using successive convex approximation (SCA). Numerical results demonstrate that the proposed joint optimization algorithm for user scheduling and resource allocation can reliably converge and achieve a higher system SE than the general multi-TRP system without carrier allocation, and this advantage is more pronounced under a higher backhaul capacity or higher power consumption constraints.

Keywords: D-MIMO system; multi-carrier system; resource allocation; user scheduling; SCA



Citation: Bu, Y.; Zong, J.; Xia, X.; Liu, Y.; Yang, F.; Wang, D. Joint User Scheduling and Resource Allocation in Distributed MIMO Systems with Multi-Carriers. *Electronics* **2022**, *11*, 1836. <https://doi.org/10.3390/electronics11121836>

Academic Editor: Luis Castedo

Received: 29 April 2022

Accepted: 7 June 2022

Published: 9 June 2022

Publisher's Note: MDPI stays neutral with regard to jurisdictional claims in published maps and institutional affiliations.



Copyright: © 2022 by the authors. Licensee MDPI, Basel, Switzerland. This article is an open access article distributed under the terms and conditions of the Creative Commons Attribution (CC BY) license (<https://creativecommons.org/licenses/by/4.0/>).

1. Introduction

The improvement of data rate is always the focus of attention in the development of wireless communication. Fifth-generation mobile communication technology, which has been deployed and implemented on a large scale, can achieve a peak data rate of 20 Gbps but has yet to be able to meet the higher demand of user-experienced data rates for 2030+ in the future [1].

Looking back on the past few decades, the vast majority of increases in communication capacity came from the densification of network infrastructure [2]. However, limited by the cell edge effect, inter-cell interference will gradually dominate as the distance between base stations decreases and will seriously effect the user-experienced data rates [3]. The D-MIMO proposed in [4] had a distributed architecture, which can effectively manage the inter-cell interference and thereby improve the network spectral efficiency and coverage [5,6].

In the D-MIMO system, multiple RAUs are distributed widely in the coverage area and connected to the baseband processing unit (BPU) via backhalls. They cooperate to

serve users by transmitting and receiving signals processed collaboratively at the central BPU, for which it can achieve higher spatial diversity/multiplexing gain [7–10].

In previous studies, user scheduling (namely user association) has always been an important research direction to improve the system efficiency in cooperation communications [11–13]. A dynamic cooperation clustering (DCC) model was proposed in [14], which constructed user-centric clustering association by setting antenna selection diagonal matrices. Considering the difference in channel quality between different users and RAUs over different carriers, the best RAUs and carriers can be matched for each user through joint optimization at the BPU, and multi-user interferences can be reduced as well.

A similar scheme, named multistream carrier aggregation (MSCA), initially appeared for heterogeneous networks, which aggregates component carriers belonging to multiple base stations for users to maximize the available configuration, thereby, improving the system data rate of service [15–17]. In [15,16], the optimization problem of energy efficiency in MSCA systems was considered by jointly investigating the user association, channel allocation and also the power allocation problems. Ref. [17] proposed a low-complexity algorithm to determine precoding vectors for MSCA systems and an efficient scheme to assign carriers to particular users based on their throughput requirements and the purpose of minimizing the total feedback overhead as well.

In addition, the discussion of resource allocation also appears in orthogonal frequency-division multi-plexing (OFDM) systems [18–20]. Ref. [18] aimed at energy-efficient power and channel allocation, along with user association optimization in OFDM systems. In [19], an iterative beamforming and scheduling strategy was proposed to maximize the system weighted sum rate, combined with the heuristic Hungarian algorithm for channel allocation on a fixed precoding pattern. However, Refs. [18,19] only considered the coordinated interference management but not the cooperative service of multiple base stations.

Most of the existing resource allocation algorithms of the distributed cooperative network do not consider multi-carrier scenarios in a coherent way or only optimize the system performance with single narrowband transmission. Though when compared with non-coherent transmissions, the coherent transmission requires strict phase synchronization across all RAUs serving a user, it can actually achieve higher system spectral efficiency with lower decoding complexity, since the non-coherent transmission needs no phase synchronization but successive interference cancellation at users to decode the individual streams [21,22]. Compared with incoherent cooperative networks, coherent cooperative networks can achieve higher system spectral efficiency [21]. However, the current research on the joint matching of users, RAUs and carriers is still confined to the traditional cellular network architecture, with restrictions on carrier selection or in a non-coherent way.

There is currently no complete resource allocation solution for a widely coordinated D-MIMO network with multi-carriers. Reasonable resource allocation and user-scheduling schemes for the coherent multi-carrier D-MIMO system are significant to improve the total spectral efficiency of D-MIMO systems. As one of the features of enhanced massive MIMO, multiple transmission and reception point (multi-TRP) can be regarded as a practical implementation of cooperative D-MIMO. In the established Release18 work package, coherent joint transmission in multi-TRP scenarios and two timing advances are listed as important evolution directions as well [23–25].

User scheduling and carrier allocation can be jointly optimized since they both belong to integer programming. Under constraints of backhaul capacity and power consumption budgets, this paper establishes a joint optimization model to solve the resource allocation and user scheduling problem in multi-TRP systems and assign appropriate RAUs and carriers to each user in a user-centric manner by setting integer matching variables. With the coherent and collaborative service provided by RAUs, the user-RAU-carrier matching variables are highly coupled in the SINR expression, making the model a non-convex and non-smooth optimization problem.

We first smooth the original problem by using penalty functions and introduce auxiliary variables to deal with the coupled variables. A concave lower bound of the objective

function is derived then, and the original problem is transformed into a series of iterative convex optimization problems by approximating the non-convex constraints with the successive convex approximation (SCA) method. Specifically, the contributions of this work are summarized as follows.

1. This paper comprehensively considers resource allocation and user scheduling for coherent multi-TRP systems with multi-carriers and generates a radio resource allocation scheme for coherently cooperative networks. We develop a mixed-integer programming model that jointly optimizes the user-RAU association and carrier allocation, as well as the downlink power allocation problems to maximize the system spectral efficiency under constraints of backhaul capacity and power consumption limits.
2. Owing to the NP-hardness of mixed-integer programming, we transform the original non-smooth non-convex optimization problem into a series of iterative convex optimization problems through penalty functions and the SCA method, and then a joint optimization algorithm of user scheduling and resource allocation for the coherent multi-TRP system with multi-carriers is proposed, of which the superiority in system spectral efficiency is verified by numerical results compared to the general multi-TRP system without channel selection.

The reminder of this paper is organized as follows. In Section 2, we give a mathematical description of the system spectral efficiency and establish a corresponding performance optimization model. In Section 3, the original optimization problem is analyzed and transformed into a tractable form, and a joint user scheduling and resource allocation algorithm is proposed. Numerical results and corresponding analysis are shown in Section 4, and the final conclusion is given in Section 5.

2. System Model and Problem Formulation

As shown in illustration Figure 1, the multi-TRP system with multi-carriers that we consider includes L single antenna RAUs, indexed by $l \in \mathcal{L} \triangleq \{1, \dots, L\}$, cooperatively serving K single antenna users, indexed by $k \in \mathcal{K} \triangleq \{1, \dots, K\}$, in a coherent way. Data signals sent by RAUs and their corresponding transmission power are uniformly determined by the central BPU, and each RAU is connected to the BPU through backhaul links. There are N available carriers in this network, indexed by $n \in \mathcal{N} \triangleq \{1, \dots, N\}$, which are reasonably assumed orthogonal to each other. Each carrier can be allocated to any user-RAU pair freely, and the specific association with RAUs and carriers of each user is scheduled by the BPU as well.

Although centralized processing will bring more computational complexity overhead to the BPU who has full knowledge of channel state information (CSI), it consequently has a better performance gain. Since RAUs are widely distributed over the coverage area in the D-MIMO system, the distance between users and RAUs is correspondingly shortened, which thereby causes better and more uniform channel conditions than that in co-located MIMO systems. We assume that the channel over each carrier between RAUs and users obeys flat fading, which means the CSI remains constant during the coherent time. Considering the tradeoff between computational complexity and system performance, we adopt the conjugate beamforming scheme as in [26], and the corresponding signal received at user k over carrier n is

$$\begin{aligned}
 y_{k,n} &= \sum_{l \in \mathcal{L}} h_{l,k,n} \sum_{k' \in \mathcal{K}} \frac{\sqrt{p_{k',n}} \rho_{l,k',n} h_{l,k',n}^* s_{k',n}}{|h_{l,k',n}|} + v_{k,n} \\
 &= \sum_{l \in \mathcal{L}} \lambda_{l,n}^{k,k} \sqrt{p_{k,n}} \rho_{l,k,n} s_{k,n} + \sum_{k' \neq k, k' \in \mathcal{K}} \sum_{l \in \mathcal{L}} \lambda_{l,n}^{k,k'} \sqrt{p_{k',n}} \rho_{l,k',n} s_{k',n} + v_{k,n}, \quad (1)
 \end{aligned}$$

where $\lambda_{l,n}^{k,k'} = \frac{h_{l,k,n} h_{l,k',n}^*}{|h_{l,k',n}|}$, $h_{l,k,n} \in \mathbb{C}$ is the channel between RAU l and user k on carrier n . $v_{k,n}$ is the complex additive white Gaussian noise (AWGN) following the distribution of $\mathcal{CN}(0, \sigma^2)$ received at user k over carrier n . $s_{k,n}$ denotes the symbol intended for user k over

carrier n , and $p_{k,n} \in \mathbb{R}$ expresses the downlink transmission power allocated for symbol $s_{k,n}$ at RAUs. It is reasonably assumed that $\{s_{k,n} | k, n \in \mathcal{K}, \mathcal{N}\}$ are independent and identically distributed variables, which are zero mean and normalized as $\mathbb{E}(|s_{k,n}|^2) = 1$. $\rho_{l,k,n} \in \{0, 1\}$ denotes the binary matching variable, which follows

$$\rho_{l,k,n} = \begin{cases} 1, & \text{if RAU } l \text{ allocates carrier } n \text{ to user } k, \\ 0, & \text{otherwise.} \end{cases} \tag{2}$$

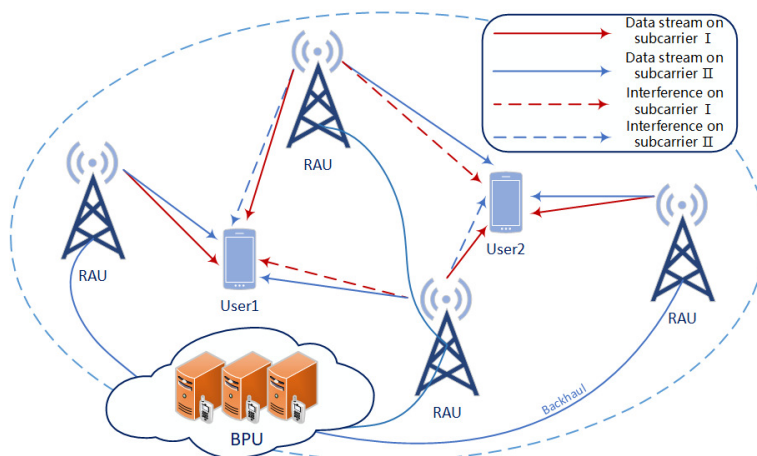


Figure 1. Illustration of the multi-TRP system with multi-carriers.

The received signal in expression (1) is illustrated as two parts, the desired signal $\sum_{l \in \mathcal{L}} \lambda_{l,n}^{k,k} \sqrt{p_{k,n}} \rho_{l,k,n} s_{k,n}$, and the interference-plus-noise term $\sum_{k' \neq k, k' \in \mathcal{K}} \sum_{l \in \mathcal{L}} \lambda_{l,n}^{k,k'} \sqrt{p_{k',n}} \rho_{l,k',n} s_{k',n} + v_{k,n}$. Clearly they are uncorrelated with each other, and thereby the signal- to-interference-plus-noise ratio (SINR) for user k over carrier n is given by

$$\gamma_{k,n} = \frac{p_{k,n} \boldsymbol{\rho}_{k,n}^H \boldsymbol{\Lambda}_n^{k,k} \boldsymbol{\rho}_{k,n}}{\sum_{k' \neq k, k' \in \mathcal{K}} p_{k',n} \boldsymbol{\rho}_{k',n}^H \boldsymbol{\Lambda}_n^{k,k'} \boldsymbol{\rho}_{k',n} + \sigma^2} \tag{3}$$

where $\boldsymbol{\rho}_{k,n} = [\rho_{1,k,n}, \rho_{2,k,n}, \dots, \rho_{L,k,n}]^T$ is the collective vector of matching variables for user k on carrier n . Let $\boldsymbol{\lambda}_n^{k,k'} = [\lambda_{1,n}^{k,k'}, \lambda_{2,n}^{k,k'}, \dots, \lambda_{L,n}^{k,k'}]$, $\boldsymbol{\Lambda}_n^{k,k'}$ is a positive semidefinite matrix formulated by $\boldsymbol{\Lambda}_n^{k,k'} = (\boldsymbol{\lambda}_n^{k,k'})^H \boldsymbol{\lambda}_n^{k,k'}$. Unlike previous studies on joint user scheduling and carrier allocation, both the numerator and denominator of Equation (3) contain a quadratic form consisting of matching variables, because with the coherent transmission all associated RAUs will transmit the same symbol to a user. Therefore, the achievable SE of user k over carrier n can be written as $R_{k,n} = \ln(1 + \gamma_{k,n})$. According to the OFDM transmission framework, the total achievable SE at user k across all available carriers is given by $R_{k,\text{total}} = \sum_{n \in \mathcal{N}} R_{k,n}$.

As can be observed in Equation (3), the SINR of each user over each carrier is determined by both the corresponding power allocation for downlink transmission at RAUs and the user-RAU-carrier three-sided matching relationships. Considering the requirement of further improving the data rate with limited frequency band resources in the future, the system spectral efficiency, which is also one of the important performance indicators in communication networks, is employed as the utility function for the optimization problem that we consider.

We denote $\boldsymbol{\Omega}$ as a $L \times K \times N$ dimensional matrix gathering elements of $\rho_{l,k,n}$ and \mathbf{P} as a $K \times N$ dimensional matrix gathering elements of $p_{k,n}$. Accordingly, the mathematical model

of the joint user scheduling and resource allocation optimization problem for a single time slot is formulated by

$$\underset{\Omega, P}{\text{maximize}} \quad \sum_{k \in \mathcal{K}} \sum_{n \in \mathcal{N}} R_{k,n} \tag{4a}$$

$$\text{subject to} \quad \text{C1: } \sum_{n \in \mathcal{N}} R_{k,n} \geq R_{\min,k}, \quad \forall k \in \mathcal{K}, \tag{4b}$$

$$\text{C2: } \sum_{n \in \mathcal{N}} \sum_{k \in \mathcal{K}} p_{k,n} \rho_{l,k,n}^2 \leq P_{\max,l}, \quad \forall l \in \mathcal{L}, \tag{4c}$$

$$\text{C3: } \sum_{n \in \mathcal{N}} \sum_{k \in \mathcal{K}} \rho_{l,k,n} R_{k,n} \leq C_{\max,l}, \quad \forall l \in \mathcal{L}, \tag{4d}$$

$$\text{C4: } \rho_{l,k,n} \in \{0, 1\}, \quad \forall l, k, n \in \mathcal{L}, \mathcal{K}, \mathcal{N}. \tag{4e}$$

In the above optimization problem (4), constraint C1 guarantees the QoS requirement for each user, and C2 and C3 restrict the maximum power consumption and backhaul budget across all frequency bands at each RAU to $P_{\max,l}$ and $C_{\max,l}$, respectively. The binary nature of the matching variable $\rho_{l,k,n}$ is ensured in C4.

Problem (4) is actually a non-convex combinatorial optimization problem, and its three-sided matching feature makes this NP-hard problem more difficult to solve. Thus, we propose an iterative optimization algorithm which transforms the original problem into a tractable form.

3. Problem Analysis and Proposed Approach

Since variable $\rho_{k,n}$ and $p_{k,n}$ are coupled together inside both the numerator and denominator of the SINR expression, the original problem is actually a complex non-convex optimization problem with combinatorial variables. Referring to [20], we first smooth the original problem by setting penalty functions, and auxiliary variables are introduced to disassemble the expression of coupled variables.

After obtaining the concave lower bound of the objective function, the SCA method is employed to transform the original non-convex problem into a series of iterative convex optimization problems, which can be easily solved. The main idea of our proposed approach is to find corresponding concave or convex approximations for the objective function and constraints, which contain parameters that have a mapping relationship with the results of the previous iteration. These parameters are constantly updated in the iterative process of solving the approximate convex optimization problem, until the solution of each iteration finally converge.

3.1. Equivalent Reformulation of Binary Constraints

The integer variable in problem (4) makes it a NP-hard problem that cannot be solved in polynomial time. According to [27], the original mixed-integer optimization problem can be transformed into a continuous form by utilizing penalty functions. We then rewrite constraint C4 as

$$\text{C5: } \rho_{l,k,n} \in [0, 1], \quad \forall l, k, n \in \mathcal{L}, \mathcal{K}, \mathcal{N}, \tag{5}$$

C5 redefines $\rho_{l,k,n}$ as a continuous variable varying within $[0, 1]$. To ensure the binary feature of the original matching variable $\rho_{l,k,n}$, penalty terms are added to the objective function, which guarantees the equivalence of the optimization problems before and after relaxation of integer variables. Referring to [27], the employed penalty function is set as

$$f(\Omega) = - \sum_{l=1}^L \sum_{k=1}^K \sum_{n=1}^N (\ln(\rho_{l,k,n} + \epsilon) + \ln((1 - \rho_{l,k,n}) + \epsilon)), \tag{6}$$

where ϵ is a very small positive constant, which can make the continuous optimization problem after transformation consistent with the original integer programming by properly setting its value. The equivalent optimization problem is then transformed into

$$\begin{aligned} & \underset{\Omega, \mathbf{P}}{\text{maximize}} && f(\Omega) + \sum_{k \in \mathcal{K}} \sum_{n \in \mathcal{N}} R_{k,n} \\ & \text{subject to} && \text{C1, C2, C3,} \\ & && \text{C5: } \rho_{l,k,n} \in [0, 1], \quad \forall l, k, n \in \mathcal{L}, \mathcal{K}, \mathcal{N}. \end{aligned} \tag{7}$$

3.2. Approximation of the Objective Function

The objective function of problem (7) comprises two parts, the achievable SE expression involving SINR $\gamma_{k,n}$ and the penalty function $f(\Omega)$, making this maximization objective function non-concave and difficult to solve. Referring to the path-following optimization algorithm in [28], the original objective function can be approximated to its concave lower bound for an iterative solution. By taking the first-order Taylor expansion of the penalty function at feasible point $\Omega^{(m)}$, the following inequality can be obtained that

$$\begin{aligned} f(\Omega) \geq \hat{f}(\Omega) = & - \sum_{l=1}^L \sum_{k=1}^K \sum_{n=1}^N \left(\ln(\rho_{l,k,n}^{(m)} + \epsilon) + \ln\left(\left(1 - \rho_{l,k,n}^{(m)}\right) + \epsilon\right) \right. \\ & \left. + \left(\frac{1}{\rho_{l,k,n}^{(m)} + \epsilon} - \frac{1}{\left(1 - \rho_{l,k,n}^{(m)}\right) + \epsilon} \right) (\rho_{l,k,n} - \rho_{l,k,n}^{(m)}) \right). \end{aligned} \tag{8}$$

This inequality relation holds because the penalty function $f(\Omega)$ is actually a concave function, and the linear function obtained by the first-order Taylor expansion at any feasible point of a concave function is greater than itself. Such inequality relation is exactly reversed for convex functions, as we shall see later. The objective function in problem (7) can then be approximated by its lower bound

$$f_{obj} = \hat{f}(\Omega) + \sum_{k \in \mathcal{K}} \sum_{n \in \mathcal{N}} R_{k,n}, \tag{9}$$

with $\hat{f}(\Omega)$ as an affine substitute for the original penalty function $f(\Omega)$. We further introduce two groups of auxiliary variables $\{x_{k,n} | x_{k,n} \in \mathbb{R}, k, n \in \mathcal{K}, \mathcal{N}\}$ and $\{y_{k,k',n} | y_{k,k',n} \in \mathbb{R}_+, k, k', n \in \mathcal{K}, \mathcal{K}, \mathcal{N}\}$ to obtain a lower bound approximation of $R_{k,n}$ in the objective function:

$$R_{k,n} \geq \bar{R}_{k,n} = \ln \left(1 + \frac{x_{k,n}^2}{\sum_{k' \neq k, k' \in \mathcal{K}} y_{k,k',n} + \sigma^2} \right), \tag{10}$$

where $x_{k,n}$ and $y_{k,k',n}$ satisfy

$$p_{k,n} \rho_{k,n}^H \Lambda_n^{k,k} \rho_{k,n} \geq x_{k,n}^2, \quad \forall k, n \in \mathcal{K}, \mathcal{N}, \tag{11}$$

$$p_{k',n} \rho_{k',n}^H \Lambda_n^{k,k'} \rho_{k',n} \leq y_{k,k',n}, \quad \forall k, k', n \in \mathcal{K}, \mathcal{K}, \mathcal{N}. \tag{12}$$

After simple transposition of terms, inequalities (11) and (12) are turned into

$$\rho_{k,n}^H \Lambda_n^{k,k} \rho_{k,n} \geq \frac{x_{k,n}^2}{p_{k,n}}, \tag{13}$$

$$\frac{\rho_{k',n}^H \Lambda_n^{k,k'} \rho_{k',n}}{y_{k,k',n}} \leq \frac{1}{p_{k',n}}. \tag{14}$$

However, after introducing additional variables, the lower bound expression $\bar{R}_{k,n}$ is still non-concave. Referring to [28,29], the following inequalities will be frequently used in the derivation below.

$$\begin{aligned} \ln\left(1 + \frac{|b|^2}{a}\right) &\geq F\left(a, b, a^{(m)}, b^{(m)}\right) \\ &= \ln\left(1 + \frac{|b^{(m)}|^2}{a^{(m)}}\right) - \frac{|b^{(m)}|^2}{a^{(m)}} + 2\frac{\Re\left\{\left(b^{(m)}\right)^* b\right\}}{a^{(m)}} - \frac{|b^{(m)}|^2\left(|b|^2 + a\right)}{a^{(m)}\left(a^{(m)} + |b^{(m)}|^2\right)}, \end{aligned} \tag{15}$$

$$\frac{1}{a} \geq \bar{F}\left(a, a^{(m)}\right) = \frac{1}{a^{(m)}} - \frac{\left(a - a^{(m)}\right)}{\left(a^{(m)}\right)^2}, \tag{16}$$

$$c^H D c \geq \hat{F}\left(c, c^{(m)}, D\right) = \left(c^{(m)}\right)^H D c^{(m)} + 2\Re\left\{\left(c^{(m)}\right)^H D\left(c - c^{(m)}\right)\right\}. \tag{17}$$

$b \in \mathbb{C}$ and $a \in \mathbb{R}_+$ in (15) and (16) are complex and positive real variables, respectively, while $b^{(m)} \in \mathbb{C}$ and $a^{(m)} \in \mathbb{R}_+$ are constants. In (17), c is a complex variable vector, and $D = d d^H$ is a positive semidefinite matrix, where d is any complex constant vector.

According to the inequality (15), a concave lower bound of $\bar{R}_{k,n}$ can be written as

$$\bar{R}_{k,n} \geq F\left(\sum_{k' \neq k, k' \in \mathcal{K}} y_{k, k', n} + \sigma^2, x_{k,n}, \sum_{k' \neq k, k' \in \mathcal{K}} y_{k, k', n}^{(m)} + \sigma^2, x_{k,n}^{(m)}\right), \tag{18}$$

which satisfies

$$F\left(\sum_{k' \neq k, k' \in \mathcal{K}} y_{k, k', n}^{(m)} + \sigma^2, x_{k,n}^{(m)}, \sum_{k' \neq k, k' \in \mathcal{K}} y_{k, k', n} + \sigma^2, x_{k,n}\right) = \ln\left(1 + \frac{\left(x_{k,n}^{(m)}\right)^2}{\sum_{k' \neq k, k' \in \mathcal{K}} y_{k, k', n}^{(m)} + \sigma^2}\right). \tag{19}$$

Similarly, following from the inequalities (17) and (16), respectively, inequalities (13) and (14) can then be approximated by

$$C6: \frac{x_{k,n}^2}{p_{k,n}} \leq \hat{F}\left(\rho_{k,n}, \rho_{k,n}^{(m)}, \Lambda_n^{k,k}\right), \quad \forall k, n \in \mathcal{K}, \mathcal{N}, \tag{20}$$

$$C7: \frac{\rho_{k',n}^H \Lambda_n^{k,k'} \rho_{k',n}}{y_{k,k',n}} \leq \bar{F}\left(p_{k',n}, p_{k',n}^{(m)}\right), \quad \forall k, k', n \in \mathcal{K}, \mathcal{K}, \mathcal{N}. \tag{21}$$

Since both the LHS of (20) and (21) are typical convex quadratic-over-linear functions, and the RHS of (20) and (21) are linear functions, it is clear that C6 and C7 are both convex constraints. By now, the objective function in problem (7) has already been approximated into a convex form, and the $(m + 1)$ -th iteration can be written as

$$\begin{aligned} &\underset{\substack{\Omega, P, \\ \{x_{k,n}, y_{k,k',n}\}_{k,k',n \in \mathcal{K}, \mathcal{K}, \mathcal{N}}}}{\text{maximize}} && \sum_{k \in \mathcal{K}} \sum_{n \in \mathcal{N}} F\left(\sum_{k' \neq k, k' \in \mathcal{K}} y_{k, k', n} + \sigma^2, x_{k,n}, \sum_{k' \neq k, k' \in \mathcal{K}} y_{k, k', n}^{(m)} + \sigma^2, x_{k,n}^{(m)}\right) + \hat{f}(\Omega) \\ &\text{subject to} && C1, C2, C3, C5, C6, C7. \end{aligned} \tag{22}$$

3.3. Convex Approximation of Constraints Involving Variable Products

Despite the above transformation of the objective function, the non-convex constraints C1, C2 and C3 still make problem (22) an intractable one. To tackle this issue, the SCA

method is utilized to approximate the non-convex constraints further. Again by employing the inequality (15), constraint C1 can be approximated by

$$C8: \sum_{n \in \mathcal{N}} F \left(\sum_{k' \neq k, k' \in \mathcal{K}} y_{k,k',n} + \sigma^2, x_{k,n}, \sum_{k' \neq k, k' \in \mathcal{K}} y_{k,k',n}^{(m)} + \sigma^2, x_{k,n}^{(m)} \right) \geq R_{\min,k}, \quad \forall k \in \mathcal{K}, \quad (23)$$

which is found to be a convex constraint due to the concavity of the LHS (left-hand side) of this inequality.

Owing to the existence of the variable product in the LHS of C2, auxiliary variables $\{\alpha_{l,k,n} | \alpha_{l,k,n} \in \mathbb{R}_+, l, k, n \in \mathcal{L}, \mathcal{K}, \mathcal{N}\}$ need to be introduced again to deal with the coupled variables, and the function $p_{k,n} \rho_{l,k,n}^2$ in C2 is upper bounded by

$$p_{k,n} \rho_{l,k,n}^2 \leq \alpha_{l,k,n}, \quad \forall l, k, n \in \mathcal{L}, \mathcal{K}, \mathcal{N}. \quad (24)$$

Thus, the original C2 can be approximated by

$$C9: \sum_{n \in \mathcal{N}} \sum_{k \in \mathcal{K}} \alpha_{l,k,n} \leq P_{\max,l}, \quad \forall l \in \mathcal{L}. \quad (25)$$

Still we need to transform the inequality (24) due to its non-convexity. After simple transposition of terms, (24) can be rewritten as

$$\frac{\rho_{l,k,n}^2}{\alpha_{l,k,n}} \leq \frac{1}{p_{k,n}}, \quad (26)$$

and both of its left- and right-hand sides (RHS) are convex functions. Following from the inequality (16), the RHS of (26) can be lower bounded by $\bar{F}(p_{k,n}, p_{k,n}^{(m)})$, which means that (26) can be approximated by

$$C10: \frac{\rho_{l,k,n}^2}{\alpha_{l,k,n}} \leq \bar{F}(p_{k,n}, p_{k,n}^{(m)}), \quad \forall l, k, n \in \mathcal{L}, \mathcal{K}, \mathcal{N}. \quad (27)$$

Since both sides of (25) are linear functions, and (27) has the same structure as C6, it is obvious that C9 and C10 are convex constraints as well.

Similar to C2, due to the existence of coupled variables, it is necessary to introduce auxiliary variables $\{t_{k,n} | t_{k,n} \in \mathbb{R}_+, k, n \in \mathcal{K}, \mathcal{N}\}$ as well. Here, we have

$$\ln \left(1 + \frac{p_{k,n} \rho_{k,n}^H \Lambda_n^{k,k} \rho_{k,n}}{\sum_{k' \neq k, k' \in \mathcal{K}} p_{k',n} \rho_{k',n}^H \Lambda_n^{k,k'} \rho_{k',n} + \sigma^2} \right) \leq t_{k,n}, \quad \forall k, n \in \mathcal{K}, \mathcal{N}, \quad (28)$$

to approximate the constraint C3 by

$$\sum_{n \in \mathcal{N}} \sum_{k \in \mathcal{K}} \rho_{l,k,n} t_{k,n} \leq C_{\max,l}, \quad \forall l \in \mathcal{L}. \quad (29)$$

However, both of (28) and (29) are yet to be convex, and thus further approximations are needed. The inequality (28) is equivalent to

$$\frac{p_{k,n} \rho_{k,n}^H \Lambda_n^{k,k} \rho_{k,n}}{\sum_{k' \neq k, k' \in \mathcal{K}} p_{k',n} \rho_{k',n}^H \Lambda_n^{k,k'} \rho_{k',n} + \sigma^2} \leq e^{t_{k,n}} - 1. \quad (30)$$

Since both the numerator and denominator in (30) contain the product of coupled variables, $\{\bar{x}_{k,n} | \bar{x}_{k,n} \in \mathbb{R}, k, n \in \mathcal{K}, \mathcal{N}\}$ and $\{\bar{y}_{k,k',n} | \bar{y}_{k,k',n} \in \mathbb{R}_+, k, k', n \in \mathcal{K}, \mathcal{K}, \mathcal{N}\}$ are introduced as auxiliary variables again, which satisfy

$$p_{k,n} \rho_{k,n}^H \Lambda_n^{k,k} \rho_{k,n} \leq \bar{x}_{k,n}^2, \quad \forall k, n \in \mathcal{K}, \mathcal{N}, \tag{31}$$

$$p_{k',n} \rho_{k',n}^H \Lambda_n^{k,k'} \rho_{k',n} \geq \bar{y}_{k,k',n}, \quad \forall k, k', n \in \mathcal{K}, \mathcal{K}, \mathcal{N}. \tag{32}$$

When the following inequality is satisfied,

$$\frac{\bar{x}_{k,n}^2}{\sum_{k' \neq k, k' \in \mathcal{K}} \bar{y}_{k,k',n} + \sigma^2} \leq e^{t_{k,n}} - 1, \tag{33}$$

the inequality (30) is also satisfied. Therefore, the LHS of (30) can be approximated by its convex upper bound function $\frac{\bar{x}_{k,n}^2}{\sum_{k' \neq k, k' \in \mathcal{K}} \bar{y}_{k,k',n} + \sigma^2}$, and after taking the first-order Taylor expansion of the RHS of (33) at a feasible point $t_{k,n}^{(m)}$, the inequality (28) can then be approximated to

$$\text{C11: } \frac{\bar{x}_{k,n}^2}{\sum_{k' \neq k, k' \in \mathcal{K}} \bar{y}_{k,k',n} + \sigma^2} \leq e^{t_{k,n}^{(m)}} + e^{t_{k,n}^{(m)}} (t_{k,n} - t_{k,n}^{(m)}) - 1, \quad \forall k, n \in \mathcal{K}, \mathcal{N}. \tag{34}$$

Inevitably, inequalities (31) and (32) also need to be transformed since they are both non-convex. After transposition, inequalities (31) and (32) are turned into

$$\rho_{k,n}^H \Lambda_n^{k,k} \rho_{k,n} \leq \frac{\bar{x}_{k,n}^2}{p_{k,n}}, \tag{35}$$

$$\frac{\rho_{k',n}^H \Lambda_n^{k,k'} \rho_{k',n}}{\bar{y}_{k,k',n}} \geq \frac{1}{p_{k',n}}. \tag{36}$$

Both of the left- and right-hand sides of (35) are convex functions, and thus an affine lower bound of the RHS of (35) can be obtained by taking its first-order Taylor expansion at feasible point $(\bar{x}_{k,n}^{(m)}, p_{k,n}^{(m)})$, and the inequality (35) can then be approximated by

$$\text{C12: } \rho_{k,n}^H \Lambda_n^{k,k} \rho_{k,n} \leq \frac{2\bar{x}_{k,n}^{(m)}}{p_{k,n}^{(m)}} \bar{x}_{k,n} - \frac{(\bar{x}_{k,n}^{(m)})^2}{(p_{k,n}^{(m)})^2} p_{k,n}, \quad \forall k, n \in \mathcal{K}, \mathcal{N}. \tag{37}$$

In (36), both the left- and right-hand sides are convex functions as well. Referring to [29], the following inequality can be used to find an affine lower bound of the LHS of (36):

$$\frac{\mathbf{c}^H \mathbf{D} \mathbf{c}}{a} \geq \tilde{F}(\mathbf{c}, \mathbf{c}^{(m)}, a, a^{(m)}, \mathbf{D}) = \frac{2\Re\left\{(\mathbf{c}^{(m)})^H \mathbf{D} \mathbf{c}\right\}}{a^{(m)}} - \frac{(\mathbf{c}^{(m)})^H \mathbf{D} \mathbf{c}^{(m)} a}{(a^{(m)})^2}, \tag{38}$$

where $a \in \mathbb{R}_+$ is a positive real variable, and $a^{(m)} \in \mathbb{R}_+$ is a constant. \mathbf{c} denotes a complex variable vector, and $\mathbf{D} = \mathbf{d} \mathbf{d}^H$ represents a positive semidefinite matrix, where \mathbf{d} can be

any complex constant vector. Following from the inequality (38), the inequality (36) can be approximated by

$$C13: \tilde{F}\left(\rho_{k',n}, \rho_{k',n}^{(m)}, \bar{y}_{k,k',n}, \bar{y}_{k,k',n}^{(m)}, \Lambda_n^{k,k'}\right) \geq \frac{1}{p_{k',n}}, \quad \forall k, k', n \in \mathcal{K}, \mathcal{K}, \mathcal{N}. \quad (39)$$

Clearly C11, C12 and C13 all have the same form of a convex function minus an affine function; thus, it is easy to see that these three constraints are all convex as well.

Now, let us focus on the inequality (29). according to the arithmetic inequality, we have [30]

$$\rho_{l,k,n} t_{k,n} \leq \frac{\psi_{l,k,n}^{(m)}}{2} \rho_{l,k,n}^2 + \frac{t_{k,n}^2}{2\psi_{l,k,n}^{(m)}}, \quad (40)$$

where the equal sign holds if and only if $\psi_{l,k,n}^{(m)} = \frac{t_{k,n}}{\rho_{l,k,n}}$. Since the RHS of (40) is convex for the fact that it contains only two convex functions adding up, the inequality (29) can be approximated by

$$C14: \sum_{n \in \mathcal{N}} \sum_{k \in \mathcal{K}} \frac{\psi_{l,k,n}^{(m)}}{2} \rho_{l,k,n}^2 + \frac{t_{k,n}^2}{2\psi_{l,k,n}^{(m)}} \leq C_{\max,l}, \quad \forall l \in \mathcal{L}. \quad (41)$$

Updating the value of $\psi_{l,k,n}^{(m)}$ in the m -th iteration according to $\psi_{l,k,n}^{(m)} = \frac{t_{k,n}^{(m)}}{\rho_{l,k,n}^{(m)}}$ can make

both sides of (40) finally equal to each other after multiple iterations.

After the transformations above, problem (22) has been completely transformed to a series of iterative convex optimization problems. The $(m + 1)$ -th iteration can be written as

$$\begin{aligned} & \underset{\substack{\Omega, P, \\ \{x_{k,n}, y_{k,k',n}, \bar{x}_{k,n}, \bar{y}_{k,k',n}, \alpha_{l,k,n}, \\ t_{k,n} | l, k, k', n \in \mathcal{L}, \mathcal{K}, \mathcal{K}, \mathcal{N}\}}} \\ & \text{maximize} \\ & \sum_{k \in \mathcal{K}} \sum_{n \in \mathcal{N}} F\left(\sum_{k' \neq k, k' \in \mathcal{K}} y_{k,k',n} + \sigma^2, x_{k,n}, \sum_{k' \neq k, k' \in \mathcal{K}} y_{k,k',n}^{(m)} + \sigma^2, x_{k,n}^{(m)}\right) + \hat{f}(\Omega) \\ & \text{subject to} \quad C5, C6, C7, C8, C9, C10, C11, C12, C13, C14. \end{aligned} \quad (42)$$

By exploiting current algorithms, such as the interior point method, the optimal solution of problem (42) can be easily obtained. With initial values reasonably set and parameters updated cyclically according to the solution of each iteration, the result of each iteration will finally converge to a local optimum. Detailed procedures of our proposed joint optimization algorithm for user scheduling and resource allocation are summarized in Algorithm 1:

Algorithm 1. Joint optimization of user scheduling and resource allocation

- 1: Set $m=0$, generate initial values of $\{\rho_{k,n}^{(m)}, p_{k,n}^{(m)}, x_{k,n}^{(m)}, y_{k,k',n}^{(m)}, \bar{x}_{k,n}^{(m)}, \bar{y}_{k,k',n}^{(m)}, t_{k,n}^{(m)}, \alpha_{l,k,n}^{(m)}, \psi_{l,k,n}^{(m)} | l, k, k', n \in \mathcal{L}, \mathcal{K}, \mathcal{K}, \mathcal{N}\}$ with constraints satisfied.
 - 2: **Repeat**
 - 3: Solve problem (42) to obtain the optimal solution $\{\rho_{k,n}^*, p_{k,n}^*, x_{k,n}^*, y_{k,k',n}^*, \bar{x}_{k,n}^*, \bar{y}_{k,k',n}^*, t_{k,n}^*, \alpha_{l,k,n}^* | l, k, k', n \in \mathcal{L}, \mathcal{K}, \mathcal{K}, \mathcal{N}\}$.
 - 4: Update parameters for the next iteration: $\rho_{k,n}^{(m+1)} = \rho_{k,n}^*, p_{k,n}^{(m+1)} = p_{k,n}^*, x_{k,n}^{(m+1)} = x_{k,n}^*, y_{k,k',n}^{(m+1)} = y_{k,k',n}^*, \bar{x}_{k,n}^{(m+1)} = \bar{x}_{k,n}^*, \bar{y}_{k,k',n}^{(m+1)} = \bar{y}_{k,k',n}^*, t_{k,n}^{(m+1)} = t_{k,n}^*, \alpha_{l,k,n}^{(m+1)} = \alpha_{l,k,n}^*, \psi_{l,k,n}^{(m+1)} = \frac{t_{k,n}^*}{\rho_{l,k,n}^*}, l, k, k', n \in \mathcal{L}, \mathcal{K}, \mathcal{K}, \mathcal{N}$.
 - 5: Set $m = m + 1$.
 - 6: **Until** Convergence
-

3.4. Complexity Analysis

It can be observed that the convex optimization problem (42) is actually a second-order cone program (SOCP), and it contains $\tilde{n} = 2LKN + 4KN + 2K^2N$ variables in total. Referring to [31], if the interior point method is used to solve this SOCP problem, the computational complexity is approximately $\mathcal{O}(\tilde{n}^{3.5})$. Given that Algorithm 1 requires T iterations to converge, the overall computational complexity can then be written as $\mathcal{O}(\tilde{n}^{3.5}T)$.

4. Numerical Results

In this section, a series of numerical simulation results are evaluated to demonstrate the effectiveness of the proposed algorithm in this paper. Compared with the general multi-TRP system without carrier resource allocation, the multi-TRP system with multi-carriers that performs dynamic resource allocation according to the CSI can achieve higher spectral efficiency gains. We consider a circular area with radius $R = 60$ m, where all RAUs are wrapped-around to avoid boundary effects, and users are randomly distributed over the coverage area and can associate with any RAU over more than one carriers. The number of RAUs is set to $L = 2$, user number $K = 4$ and available carrier number $N = 2$. The following channel coefficient model is considered:

$$h_{l,k,n} = \sqrt{\beta_{l,k,n}}g_{l,k,n}, \tag{43}$$

where $g_{l,k,n} \sim \mathcal{CN}(0, 1)$ is the small scale fading coefficient, and $\beta_{l,k,n}$ is the large scale fading coefficient involving path loss and shadowing effects, which would be modeled by

$$10\log_{10}(\beta_{l,k,n}) = -128.1 - 37.6\log_{10}(d_{l,k}) + x_{l,k,n}, \tag{44}$$

where $d_{l,k}$ denotes the distance between RAU l and user k in kilometers, and $x_{l,k,n} \sim \mathcal{N}(0, \sigma_{\text{shad}}^2)$ is the shadow fading with $\sigma_{\text{shad}} = 8$ dB. The noise power at receivers is given by $\sigma^2 = 10^{(n_d - 30)/10}B$, where $n_d = -174$ dBm/Hz is the noise power density, and B is the single carrier bandwidth. The total frequency bandwidth of the system is $NB = 10$ MHz.

Without loss of generality, the relative stopping criteria of the proposed algorithm is set to 5×10^{-5} , and the maximum iteration number is set to 60 to ensure sufficient convergence. When the maximum power consumption budget at each RAU set to 10 mW, under different backhaul capacity limits of 50, 100 and 150 Mbps, convergence of the proposed joint optimization algorithm for user scheduling and resource allocation is demonstrated in Figure 2.

As can be seen, all gradually increasing curves of the total spectral efficiency of the multi-carrier multi-TRP system finally converge to a stable value within about seven to eight iterations. Driven by the penalty function, the matching variables will eventually converge to 0/1 binary forms.

Figure 3 compares the system spectral efficiency of multi-TRP systems with and without carrier allocation under different settings. Figure 3a depicts carvers of system spectral efficiency versus transmission power limit P_{max} under backhaul capacity constraints of 100 Mbps and 150 Mbps. It can be seen that, with the increase of the power consumption limit at each RAU, the system spectral efficiency of both systems also increases and gradually flattens out.

Furthermore, with different power consumption constraints, the total spectral efficiency of the multi-TRP system with multi-carriers using the proposed joint optimization algorithm of user scheduling and resource allocation is always higher than that of the general multi-TRP system without carrier allocation. This advantage also increases with the growth of power consumption limits. With the power consumption budget set to 20 mW, compared with the general multi-TRP system without carrier allocation, our proposed joint

optimization algorithm can help the multi-TRP system with multi-carriers achieve over 6% performance gain of the total spectral efficiency.

In Figure 3b, how the system spectral efficiency changes with the growth of the backhaul capacity limit under different power consumption budgets is demonstrated. We investigate the impact of different backhaul capacity limits from 80 to 200 Mbps on the system spectral efficiency under power consumption budgets set to 50 and 500 mW. Consistent with general inferences, as the backhaul capacity limit increases, the total spectral efficiency of both multi-TRP systems with and without carrier allocation increases accordingly as well, and each increasing curve will gradually level off owing to the restriction from other radio resource settings. As can be seen, the upper limit of system spectral efficiency under the power consumption budget of 500 mW is apparently higher than that of 50 mW.

In addition, the multi-carrier multi-TRP system with the proposed joint optimization algorithm can always achieve higher system spectral efficiency than that of the general multi-TRP system without carrier allocation under different backhaul capacity constraints, and such gaps also grow as the backhaul capacity constraint increases. Under the backhaul capacity limit of 200 Mbps, the proposed joint optimization algorithm for user scheduling and resource allocation can bring about 6% performance gain.

Figure 4 depicts when P_{max} is set to 5 W, the system spectral efficiency of the proposed algorithm versus the number of users under different backhaul capacity limits set to 100, 120 and 150 Mbps. It can be observed from Figure 4 that the system spectral efficiency grow with the number of users since the proposed algorithm can exploit multiuser diversity brought by the CSI-based joint user scheduling and carrier allocation. Such result is consistent with the general conclusion.

We further compare the performance between the proposed optimization algorithm and another benchmark using the genetic algorithm (GA) for the joint user scheduling and carrier allocation. As a heuristic algorithm, GA is also one of the popular algorithms for integer programming. Figure 5 shows the superiority of our proposed algorithm over GA, with P_{max} set to 50 mW. The system spectral efficiency of the optimization algorithm proposed in this paper is higher than that of GA under different backhaul constraints, and the advantage is more obvious when the backhaul capacity limit is small.

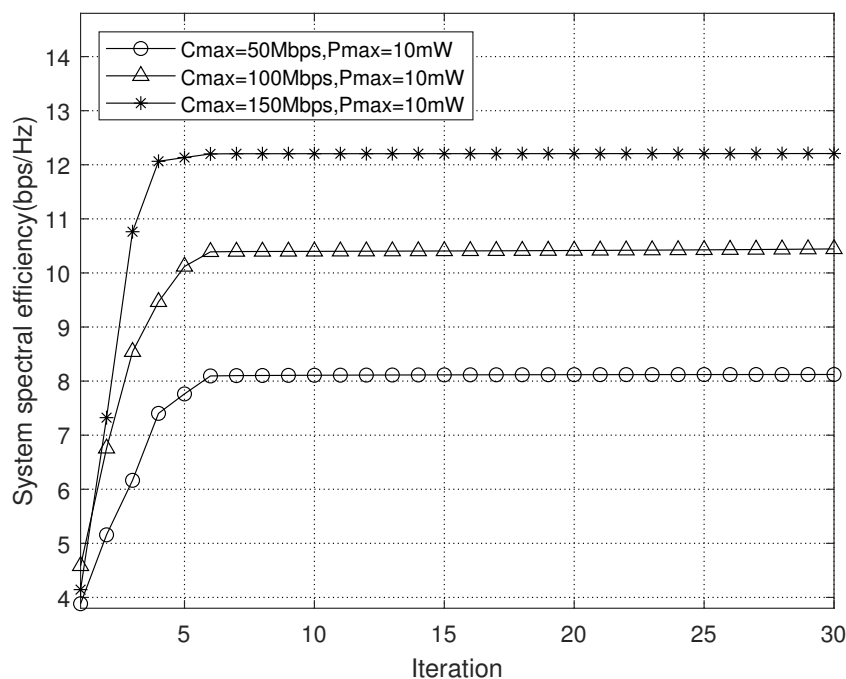
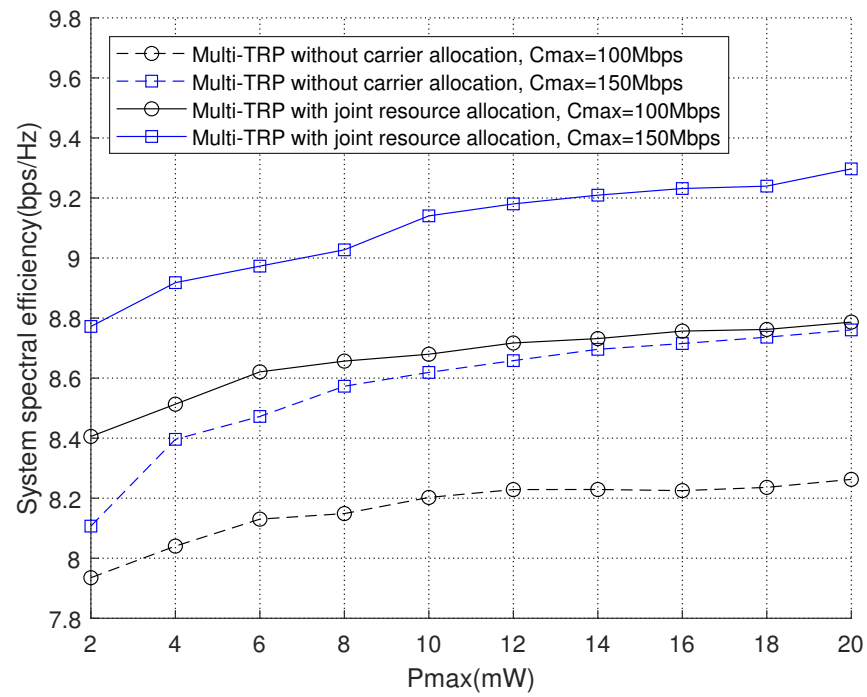
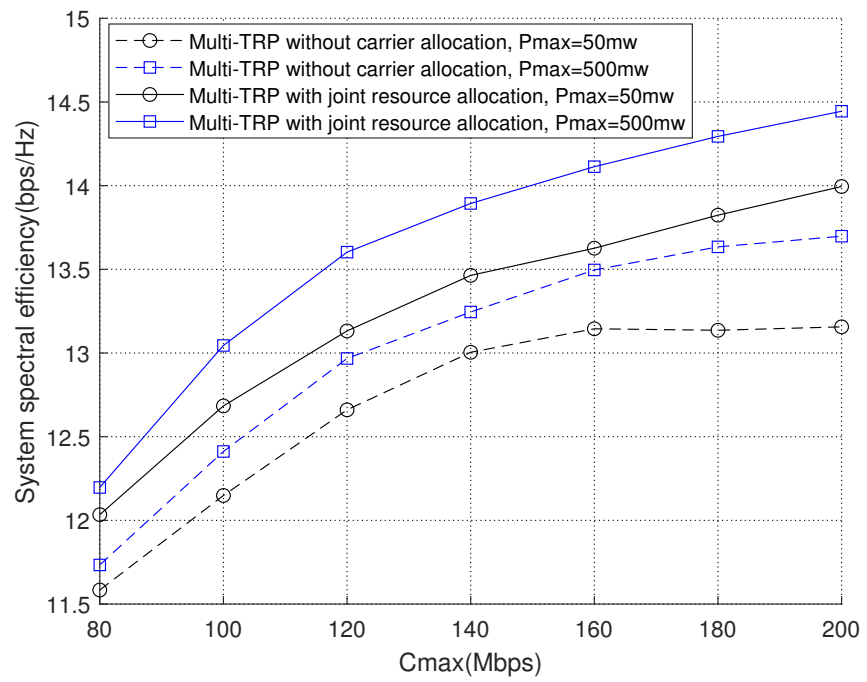


Figure 2. Convergence of the joint optimization algorithm for user scheduling and resource allocation.



(a)



(b)

Figure 3. System SE comparison of the multi-TRP systems with and without carrier allocation. (a) System SE versus P_{max} for different C_{max} limitations. (b) System SE versus C_{max} for different P_{max} limitations.

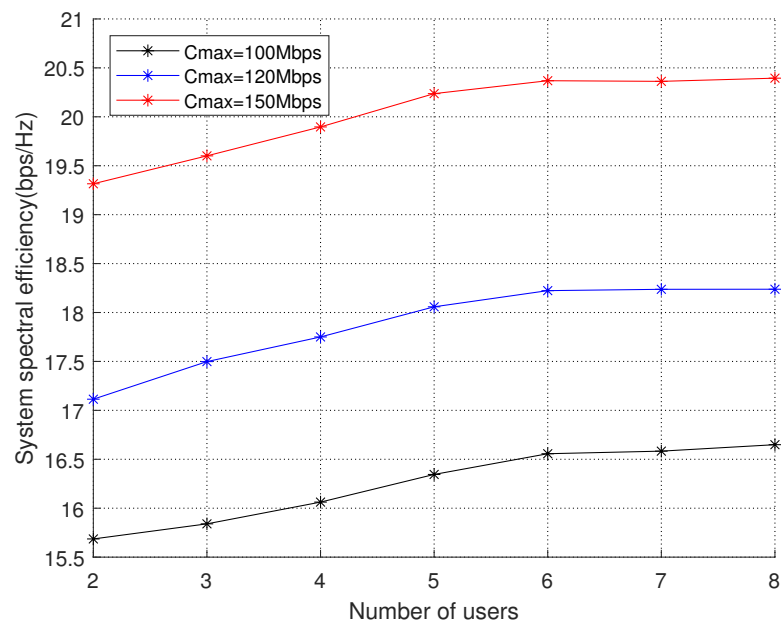


Figure 4. System SE versus the number of users for different C_{max} limitations.

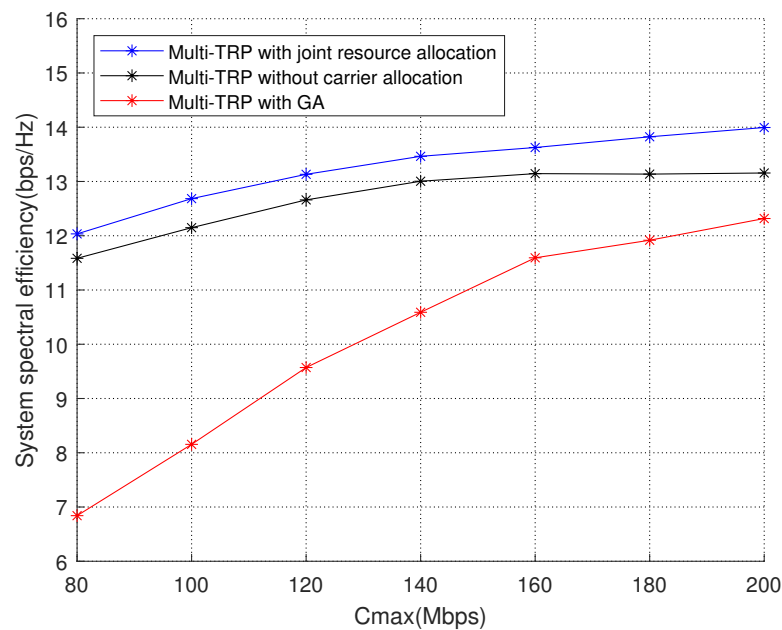


Figure 5. Performance comparison between the proposed algorithm and GA.

5. Conclusions

In this paper, we considered a coherent multi-TRP system with multi-carriers, where RAUs collaboratively serve the users in a coherent way and users are allowed to associate with any RAU over each carrier freely. In order to maximize the system spectral efficiency, we established a joint optimization problem of user-RAU-carrier three-sided matching and downlink transmission power allocation for the coherent multi-carrier multi-TRP system under the constraints of power consumption and backhaul capacity limits at each RAU, as well as the QoS requirement at each user.

Due to the existence of integer variables and the products of coupled variables, the original problem is both non-convex and non-smooth and thus intractable. In this paper, a joint optimization algorithm of user scheduling and resource allocation was proposed to tackle this problem.

By employing penalty functions and the SCA method, the original non-convex combinatorial optimization problem was transformed into a series of iterative convex optimization problems that could be easily solved. Numerical results also confirmed that, with the same settings, the multi-carrier multi-TRP system with the proposed joint optimization algorithm of user scheduling and resource allocation was able to achieve higher system spectral efficiency compared with the multi-TRP system without carrier allocation.

Author Contributions: Conceptualization, Y.B. and X.X.; Formal analysis, Y.B. and X.X.; Funding acquisition, D.W.; Methodology, Y.B. and X.X.; Project administration, Y.L. and F.Y.; Software, Y.B.; Supervision, J.Z.; Validation, Y.B.; Writing—original draft, Y.B.; Writing—review and editing, Y.B. and X.X. All authors have read and agreed to the published version of the manuscript.

Funding: This work was supported in part by the National Key Research and Development Program under Grant 2020YFB1807200, the National Natural Science Foundation of China (NSFC) under Grant 61871122, the Support Plan for Postdoctoral Talents in Jiangsu Province and the Project funded by the China Postdoctoral Science Foundation under Grant No. 2021M702500.

Data Availability Statement: Not applicable.

Conflicts of Interest: The authors declare no conflict of interest.

References

1. You, X.; Wang, C.X.; Huang, J.; Gao, X.; Zhang, Z.; Wang, M.; Huang, Y.; Zhang, C.; Jiang, Y.; Wang, J.; et al. Towards 6G wireless communication networks: Vision, enabling technologies, and new paradigm shifts. *Sci. China Inf. Sci.* **2021**, *64*, 1–74. [[CrossRef](#)]
2. Zhang, J.; Björnson, E.; Matthaiou, M.; Ng, D.W.K.; Yang, H.; Love, D.J. Prospective multiple antenna technologies for beyond 5G. *IEEE J. Sel. Areas Commun.* **2020**, *38*, 1637–1660. [[CrossRef](#)]
3. You, X.; Wang, D.; Wang, J. *Distributed MIMO and Cell-Free Mobile Communication*; Springer: Berlin/Heidelberg, Germany, 2021.
4. Roh, W.; Paulraj, A. MIMO channel capacity for the distributed antenna. In Proceedings of the IEEE 56th Vehicular Technology Conference, Vancouver, BC, Canada, 24–28 September 2002; IEEE: Piscataway, NJ, USA, 2002; Volume 2, pp. 706–709.
5. Wang, D.; Wang, J.; You, X.; Wang, Y.; Chen, M.; Hou, X. Spectral efficiency of distributed MIMO systems. *IEEE J. Sel. Areas Commun.* **2013**, *31*, 2112–2127. [[CrossRef](#)]
6. Choi, W.; Andrews, J.G. Downlink performance and capacity of distributed antenna systems in a multicell environment. *IEEE Trans. Wirel. Commun.* **2007**, *6*, 69–73. [[CrossRef](#)]
7. Zhu, P.; Bao, J.; Zhang, L.; Li, J. A pilot allocation algorithm based on coalitional game theory for distributed MIMO systems. *IEEE Access* **2019**, *7*, 105996–106001. [[CrossRef](#)]
8. Li, J.; Wang, D.; Zhu, P.; You, X. Impacts of practical channel impairments on the downlink spectral efficiency of large-scale distributed antenna systems. *Sci. China Inf. Sci.* **2019**, *62*, 1–14. [[CrossRef](#)]
9. Li, J.; Lv, Q.; Yang, J.; Zhu, P.; You, X. Spectral and Energy Efficiency of Distributed Massive MIMO with Low-Resolution ADC. *Electronics* **2018**, *7*, 391. [[CrossRef](#)]
10. Lv, Q.; Li, J.; Zhu, P.; Wang, D.; You, X. Downlink Spectral Efficiency Analysis in Distributed Massive MIMO with Phase Noise. *Electronics* **2018**, *7*, 317. [[CrossRef](#)]
11. Dao, H.T.; Kim, S. Power Allocation and User-AP Connection in Distributed Massive MIMO Systems. *IEEE Commun. Lett.* **2020**, *25*, 565–569. [[CrossRef](#)]
12. Seki, Y.; Saito, T.; Adachi, F. A study on UE clustering and antenna selection for distributed MIMO cooperative transmission using multi-user MMSE-SVD. In Proceedings of the 2019 25th Asia-Pacific Conference on Communications (APCC), Ho Chi Minh City, Vietnam, 6–8 November 2019; IEEE: Piscataway, NJ, USA, 2019; pp. 73–77.
13. Dong, G.; Zhang, H.; Jin, S.; Yuan, D. Energy-efficiency-oriented joint user association and power allocation in distributed massive MIMO systems. *IEEE Trans. Veh. Technol.* **2019**, *68*, 5794–5808. [[CrossRef](#)]
14. Björnson, E.; Jalden, N.; Bengtsson, M.; Ottersten, B. Optimality properties, distributed strategies, and measurement-based evaluation of coordinated multicell OFDMA transmission. *IEEE Trans. Signal Process.* **2011**, *59*, 6086–6101. [[CrossRef](#)]
15. Chen, Q.; Yu, G.; Yin, R.; Li, G.Y. Energy-efficient user association and resource allocation for multistream carrier aggregation. *IEEE Trans. Veh. Technol.* **2015**, *65*, 6366–6376. [[CrossRef](#)]
16. Chavarria-Reyes, E.; Akyildiz, I.F.; Fadel, E. Energy-efficient multi-stream carrier aggregation for heterogeneous networks in 5G wireless systems. *IEEE Trans. Wirel. Commun.* **2016**, *15*, 7432–7443. [[CrossRef](#)]
17. Tsinos, C.; Galanopoulos, A.; Foukalas, F. Low-complexity and low-feedback-rate channel allocation in CA MIMO systems with heterogeneous channel feedback. *IEEE Trans. Veh. Technol.* **2016**, *66*, 4396–4409. [[CrossRef](#)]
18. Venturino, L.; Zappone, A.; Risi, C.; Buzzi, S. Energy-efficient scheduling and power allocation in downlink OFDMA networks with base station coordination. *IEEE Trans. Wirel. Commun.* **2014**, *14*, 1–14. [[CrossRef](#)]
19. Khan, A.A.; Adve, R.S.; Yu, W. Optimizing downlink resource allocation in multiuser MIMO networks via fractional programming and the hungarian algorithm. *IEEE Trans. Wirel. Commun.* **2020**, *19*, 5162–5175. [[CrossRef](#)]

20. Zarandi, S.; Khalili, A.; Rasti, M.; Tabassum, H. Multi-objective energy efficient resource allocation and user association for in-band full duplex small-cells. *IEEE Trans. Green Commun. Netw.* **2020**, *4*, 1048–1060. [[CrossRef](#)]
21. Ammar, H.A.; Adve, R.; Shahbazpanahi, S.; Boudreau, G.; Srinivas, K.V. Downlink resource allocation in multiuser cell-free MIMO networks with user-centric clustering. *IEEE Trans. Wirel. Commun.* **2021**. [[CrossRef](#)]
22. Pan, C.; Ren, H.; Elkashlan, M.; Nallanathan, A.; Hanzo, L. The non-coherent ultra-dense C-RAN is capable of outperforming its coherent counterpart at a limited fronthaul capacity. *IEEE J. Sel. Areas Commun.* **2018**, *36*, 2549–2560. [[CrossRef](#)]
23. Muruganathan, S.; Faxer, S.; Jarmyr, S.; Gao, S.; Frenne, M. On the system-level performance of coordinated multi-point transmission schemes in 5G NR deployment scenarios. In Proceedings of the 2019 IEEE 90th Vehicular Technology Conference (VTC2019-Fall), Honolulu, HI, USA, 22–25 September 2019; IEEE: Piscataway, NJ, USA, 2019; pp. 1–5.
24. Shi, Z.; Chen, W.; Huang, Y.; Tian, J.; Fang, Y.; You, X.; Guo, L. Multiple-input multiple-output enhancement and beam management. In *5G NR and Enhancements*; Elsevier: Amsterdam, The Netherlands, 2022; pp. 413–506.
25. Lin, X. An Overview of 5G Advanced Evolution in 3GPP Release 18. *arXiv* **2022**, arXiv:2201.01358.
26. Nasir, A.A.; Tuan, H.D.; Ngo, H.Q.; Duong, T.Q.; Poor, H.V. Cell-free massive MIMO in the short blocklength regime for URLLC. *IEEE Trans. Wirel. Commun.* **2021**, *20*, 5861–5871. [[CrossRef](#)]
27. Lucidi, S.; Rinaldi, F. Exact penalty functions for nonlinear integer programming problems. *J. Optim. Theory Appl.* **2010**, *145*, 479–488. [[CrossRef](#)]
28. Nguyen, V.D.; Duong, T.Q.; Tuan, H.D.; Shin, O.S.; Poor, H.V. Spectral and energy efficiencies in full-duplex wireless information and power transfer. *IEEE Trans. Commun.* **2017**, *65*, 2220–2233. [[CrossRef](#)]
29. Xia, X.; Zhu, P.; Li, J.; Wu, H.; Wang, D.; Xin, Y. Joint optimization of spectral efficiency for cell-free massive MIMO with network-assisted full duplexing. *Sci. China Inf. Sci.* **2021**, *64*, 1–16. [[CrossRef](#)]
30. Beck, A.; Ben-Tal, A.; Tretuashvili, L. A sequential parametric convex approximation method with applications to nonconvex truss topology design problems. *J. Glob. Optim.* **2010**, *47*, 29–51. [[CrossRef](#)]
31. Ye, Y. *Interior Point Algorithms: Theory and Analysis*; John Wiley & Sons: Hoboken, NJ, USA, 2011; Volume 44.